Available online at www.sciencedirect.com
ScienceDirect
Journal of Nuclear Materials 357 (2006) 1–8
journal of nuclear materials
www.elsevier.com/locate/jnucmat

H, He, Ne, Ar-bombardment of amorphous hydrocarbon structures

P. Träskelin *, K. Nordlund, J. Keinonen

Association EURATOM-Tekes, Accelerator Laboratory, University of Helsinki, P.O. Box 43, Pietari Kalmin k. 2, 00014 Helsinki, Finland

Received 7 June 2005; accepted 20 December 2005

Abstract

Amorphous hydrogenated carbon films have found various applications due to the unique combination of properties of this material. In tokamak-like fusion reactors, this material is subject to bombardment primarily by H, but also to smaller amounts of noble gas ions. The effect of these low energy noble gas ions on the erosion of carbon is however not known. In this work, both cumulative and non-cumulative bombardment simulations were performed of hydrogen, helium, neon, and argon ions impinging onto a-C:H surfaces at energies ranging from 2 to 10 eV, employing a reactive hydrocarbon potential model. At noble gas/hydrogen ratios of 1/10 we saw no significant difference between the sputtering yields obtained from the bombardment simulations of different noble gas ions. A marked difference in the surface morphology was, however, observed between the final simulation cells from the 5 eV and the 10 eV ion bombardment simulations.

PACS: 82.20.Wt; 79.20.Ap; 34.50.Dy; 52.40.Hf

1. Introduction

The interest in amorphous hydrogenated carbon (a-C:H) layers has been continuously increasing during the last decades. One of the most technically and scientifically challenging applications of these materials is the use of carbon-based coatings as a protective surface for the first wall structures in tokamak fusion devices. Due to the excellent plasma facing properties, carbon-based materials are promising candidates for coating the divertor plates, and hydrogenated carbon-based materials will most probably be produced at the surface in ITER through interaction with the boundary plasma [1]. The main drawback of using carbon as a first wall material has, however, proven to be the co-deposition of tritium and the chemical erosion caused by the impacts of low-energy (1–100 eV) hydrogen ions and neutrals escaping from the core plasma. This is an important application of energetic particle-surface interaction theory in the prediction of the erosion of tokamak fusion reactor walls.

The erosion mechanisms of carbon at low plasma temperatures, that is, low ion impact energies, can principally be classified as chemical sputtering. This denotes the ejection of molecular species from the

* Corresponding author. Tel.: +358 9 191 50088; fax: +358 9 191 50042.
E-mail address: petra.traskelin@helsinki.fi (P. Träskelin).

0022-3115/$ - see front matter © 2006 Elsevier B.V. All rights reserved.
doi:10.1016/j.jnucmat.2005.12.004

surface as a result of formation and breaking of chemical bonds. Carbon based plasma facing components are also very efficiently eroded by oxygen with the formation of carbon oxides. With a selection of good gettering materials in the first wall, the effect of oxygen can, however, be suppressed, in contrast to the intense flux of low-energy hydrogen which always is present.

Another major issue to be dealt with in the design of plasma facing components is the erosion of carbon surfaces by impurity ions, i.e., ions which are not the main plasma constituents, hydrogen, deuterium or tritium. These ions, the most important ones being argon, neon and helium, will not only erode the carbon surface but also penetrate it. Mixed layers which are formed with different carbon/ion ratios could be re-eroded by incoming hydrogen ions. Therefore, the erosion behavior of these layers should be studied during the deposition of hydrogen.

The aim of the current work is to obtain an understanding of whether and how the noble gas ions affect the buildup of hydrogen and carbon erosion from a-C:H plasma facing materials.

In our previous works of hydrogen bombardment onto a-C:H surfaces [2–5], we have shown that carbon molecules can erode from a-C:H by the swift chemical sputtering mechanism, where low-energy ($\geqslant 2$ eV) hydrogen ions penetrate between two carbon atoms, which can cause chemical bonds to break and thus lead to erosion of hydrocarbon molecules. In simulations of prolonged H bombardment, the predominant hydrogen erosion mechanism for low H fluences was ion reflection from the surface [4,5]. When the dose increased, the ion reflection decreased and the sputtering of hydrogen molecules became more and more frequent. The number of hydrogen atoms in the a-C:H cell increased rapidly during the first 500–1000 impact events, and eventually reached a steady-state. Due to replacement collisions, driving surface hydrogen deeper into the cell, small increments occurred after ~2000 impact events. Since the H/C ratios in the simulation cells were clearly higher than the bulk saturation value of ~0.4, the concentration due to the high-flux bombardment was designated the term *supersaturated*. The high hydrogen content lead to the shielding of carbon atoms from new incoming hydrogen ions, and thus a decrease of roughly an order of magnitude in the carbon erosion yield.

Reduced carbon erosion yields at extremely high flux densities ($\sim 10^{22}$–10^{23} m^{-2} s^{-1}) have been reported both in tokamaks [6–9] and in plasma simulators [10]. The data for the flux dependence were recently reviewed by Roth et al. [11]. The assumption that the carbon erosion yield Y_C is dependent on the ion flux density Γ as $Y_C = \Gamma^{-\alpha}$, has given α values of ~0.4–1.25. Since the ion fluxes onto the divertor plates in ITER are estimated to be as high as 10^{24} m^{-2} s^{-1} this effect could be favorable to the use of carbon in these plates. The supersaturated hydrogen concentration at the surface is a reasonable explanation for this flux dependence of the C erosion yield in tokamak and plasma simulator experiments.

2. Simulation method

The bombardment of hydrogen and noble gas ions onto a-C:H surfaces was performed by means of MD simulations. We employed the reactive bond-order potential energy function due to Brenner–Beardmore in its second parameterization [12] in order to model the hydrogen and carbon interactions in our simulations. This potential provides a reasonable description of the bulk phases of carbon and the changes in atomic hybridization due to chemical reactions. Many studies involving interactions of hydrocarbons with carbon surfaces have therefore been carried out using this potential [13–17]. Moreover, a large advantage in using an empirical force model such as this one is that it is computationally much more efficient than quantum mechanical force models. This enables us to deal with system sizes and time scales relevant in the present study. Although this model is not as accurate as quantum-mechanical methods, it retains the essential characteristics of the chemical bond. In our simulations the equations of motion were solved using a fifth-order predictor–corrector Gear algorithm, and the scaling methods of Berendsen et al. [18] were used for the temperature and pressure control.

The creation of a-C:H cells to be used in our bombardment simulations consisted basically of four different phases: construction of random cells, annealing of the cells in order to find stable structures, attaining desired carbon coordination fractions, and creation of surfaces. A total of 4 simulation cell samples with slightly different compositions were created in order to improve the statistical significance of our results.

In the initial sample manufacturing phase 1000 atoms were randomly distributed in a box with the

dimensions $15 \times 15 \times 30$ Å. In order to match the experimentally observed saturation value at 300 K [20,19] the hydrogen–carbon ratio was aimed to be about 0.4. We ensured that the minimum separation was at least 1.5 Å between the carbon atoms, and 1.1 Å between carbon and hydrogen atoms. After this, annealing of the cell was done in order to find a stable structure. Periodic boundary conditions were applied in all directions, and the cell was equilibrated at temperatures of ~4000 K. By quenching the cell to 0 K, the lowest possible energy configuration for the structure was achieved. In order to overcome possible potential barriers a few more runs at lower temperatures ~1000 K were done. The desired sp^2 and sp^3 bonding fractions for the carbon atoms were then achieved by placing the cells under high pressures of ~10–1000 kbar. After this, the samples were relaxed once more at zero pressure and temperature. Removal of the periodic boundary conditions in one direction was done in order to create a free surface, and atoms within a distance of 2 Å of the bottom of the cell were fixed in order to imitate a bulk layer underneath. The cell was eventually equilibrated at 300 K for 50 ps so that artificially broken bonds could be cured. After this procedure physically sensible sp^2–sp^3 ratios and a stable surface was obtained. The calculated values for the final densities of the different cells were ~2.4 g/cm^3 and the fraction of the three- and four-fold coordinated carbon atoms ranged between 60%–70% and 25%–40%, respectively. One of the original surfaces is depicted in Fig. 1(a).

The bombardment simulations were commenced by placing a noble gas or hydrogen atom above the cell surface, at a distance larger than the cutoff radius of the model. The atom was assigned a speed equivalent to 2, 3, 4, 5 or 10 eV, and aimed at the surface at a normal angle of incidence. The surface was uniformly sampled and the point of impact was chosen randomly.

In this study we performed two main sets of ion bombardment simulation runs: *cumulative* and *non-cumulative*. In the cumulative bombardment simulations the cell from a previous run was used in every new simulation run. This line of action allowed us to mimic a-C:H layers being bombarded several times and to investigate the hydrogen build-up at the surface. Species that had been sputtered, that is species not bound to the surface with covalent bonds in the end of the simulation, were removed and the cell was relaxed at a temperature of 300 K before the next ion was launched toward the surface. Cumulative simulation runs were carried out for ions with energies of 5 and 10 eV in the following cases: 90% H + 10% Ar, 90% H + 10% Ne, 90% H + 10% He, 100% Ar, 100% Ne and 100% He. Additionally pure H bombardment simulations were performed for the ion energies 2, 3, 4, 5 and 10 eV. We employed various initial boxes for each combination of ion energy and species in order to obtain statistically significant results.

In our non-cumulative runs the same initial cell was used for every incident ion. As target cells, we employed a-C:H cells obtained after 0 (the original, unsaturated cell), 500 and 2000 cumulative bombardment simulations of both pure H and H + 10% Ar ion impacts. These target surfaces were then used in non-cumulative simulations of 100% H and H + 10% Ar ion bombardment simulations, where the ions were given energies of 5 and 10 eV.

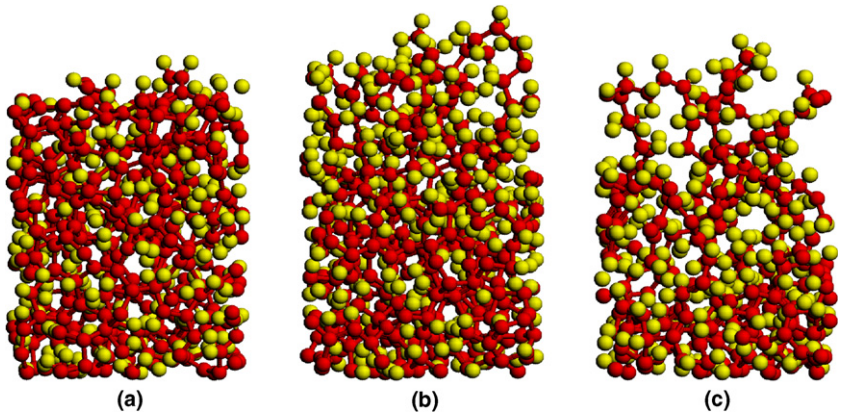

Fig. 1. Snapshots over the original surface (a), and surfaces after 3000 cumulative bombardment simulations of 5 eV (b) and 10 eV (c) impinging hydrogen ions.

The simulation runs consisted of up to 10 000 ion impacts, and each ion bombardment was simulated for 5 ps. In the cumulative bombardment simulations the cell was additionally relaxed for 5 ps between every simulation run. We employed mono-energetic irradiation in all simulations with 5 and 10 eV ions. A Maxwell–Boltzmann energy distribution was additionally used to set the energy of hydrogen ions in the pure hydrogen cumulative bombardment simulations, where the ions had energies of 2, 3, 4, 5 and 10 eV, in order to investigate the differences between these two energy distributions. Detailed analyses of the evolution of hydrogen and carbon atoms in the cell as well as the types and the numbers of the sputtered species were performed at the end.

3. Results

3.1. Co-bombardment with noble gases

The carbon erosion yields obtained from our 10 eV hydrogen and noble gas cumulative ion bombardment simulations ranged from $(36 \pm 5) \times 10^{-3}$ to $(30 \pm 5) \times 10^{-3}$ for pure hydrogen and hydrogen co-bombardment with helium, neon and argon, see Table 1. Calculated carbon sputtering yields in the 5 eV ion bombardments ranged from $(6 \pm 2) \times 10^{-3}$ to $(8 \pm 2) \times 10^{-3}$. Within the statistical uncertainties, the erosion yield does not differ for different noble gas ions.

In the simulations with 100% H impinging at energies of 2, 3, 4, 5, and 10 eV the erosion yield approached zero when the ion energy was decreasing (see Figs. 2 and 3). In these simulations the energy was set by means of a Maxwell–Boltzmann energy distribution. By comparing the erosion yield at 5 eV $(8 \pm 2) \times 10^{-3}$ to the erosion yield obtained from the 5 eV simulations with mono-energetic irradiation, $(7 \pm 2) \times 10^{-3}$, we can state that these values do not differ within the statistical uncertainties.

Table 1
Carbon sputtering yields obtained from cumulative bombardment simulations of 5 and 10 eV pure hydrogen and hydrogen co-bombardment with different noble gases

Ions	Carbon sputtering yields	
	5 eV (10^{-3})	10 eV (10^{-3})
100% H	7 ± 2	36 ± 5
H + 10% He	7 ± 2	34 ± 5
H + 10% Ne	8 ± 2	31 ± 5
H + 10% Ar	6 ± 2	30 ± 5

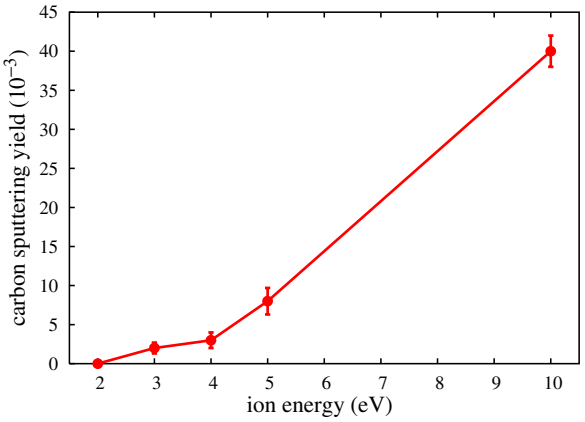

Fig. 2. Carbon sputtering yields obtained from cumulative bombardment simulations with hydrogen. The energies of incident particles were distributed according to a Maxwell–Boltzmann distribution.

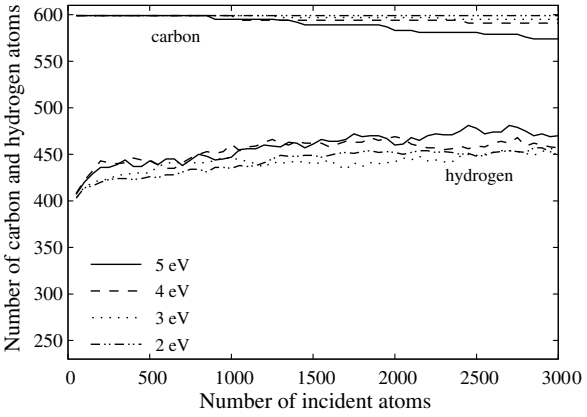

Fig. 3. Evolution of carbon and hydrogen atoms in the samples during cumulative bombardment simulations with hydrogen. The energies of incident particles were distributed according to a Maxwell–Boltzmann distribution.

The evolution of the number of carbon and hydrogen atoms in the samples during bombardment of only hydrogen as well as hydrogen in combination with argon, neon and helium at ions energies of 5 and 10 eV, is depicted in Figs. 4 and 5. After ~2500 events we see that the number of hydrogen atoms starts to decrease in all simulations where the ion energy is 10 eV. Overall, cells with smaller hydrogen content in the beginning of the simulation were seen to reach a saturated state later than cells with a large initial hydrogen content.

The predominant hydrogen erosion mechanism at the start of the cumulative simulations was ion reflection from the surface [3,5]. When the buildup increased, the reflection of the incoming hydrogen

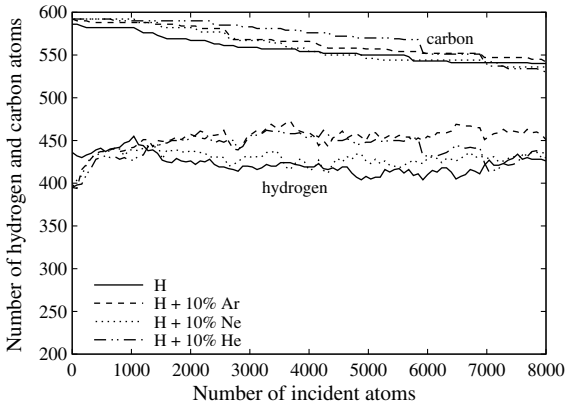

Fig. 4. Evolution of carbon and hydrogen atoms in the samples during cumulative bombardment simulations with hydrogen, as well as hydrogen in combination with noble gas atoms. The energy of an incident particle was 5 eV (mono-energetic irradiation).

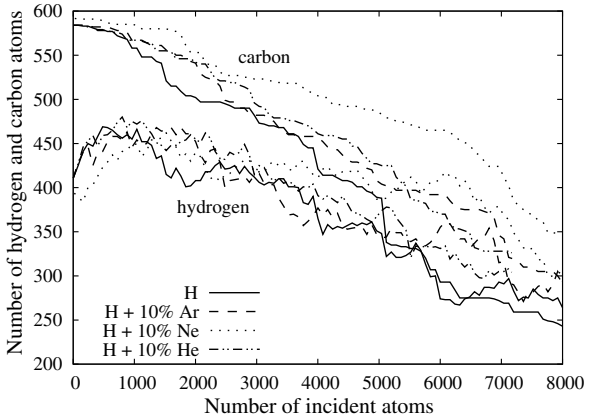

Fig. 5. Evolution of carbon and hydrogen atoms in the samples during cumulative bombardment simulations with hydrogen, as well as hydrogen in combination with noble gas atoms. The energy of an incident particle was 10 eV (mono-energetic irradiation).

ions decreased and the sputtering of hydrogen molecules became more and more frequent. The ion flux was high enough to result in saturation of hydrogen at the surface.

The hydrogen erosion begins when no additional hydrogen supersaturation can take place and the erosion of carbon starts to become significant. In the 5 eV cumulative ion bombardment simulations the number of hydrogen atoms in the cell remains on a constant level. The 5 eV ions do not penetrate deep into the sample which means that a dense surface layer which is hard to erode will be formed. The 10 eV ions, however, penetrate deeper, leading to the formation of loosely bound hydrocarbons. In Fig. 1 the uppermost part (surface) of the simulation box is depicted from snapshots of the original simulation cell, and the simulation cell after 3000 cumulative bombardment simulations of 5 eV and 10 eV impinging hydrogen ions.

In the non-cumulative simulations we also obtained higher hydrogen and carbon erosion yields from the simulations with higher ion energies. Since one single surface is used in one set of simulation runs in these simulations, the result will be highly dependent on what the surface configuration of this selected cell happens to be, and one could expect the result to differ a lot between different simulation runs. This is why we considered the cumulative simulations more reliable for obtaining a sputtering yield than the non-cumulative.

3.2. 100% noble gas bombardment

Since no difference was observed between the cumulative bombardment simulations with 0 and 10% noble gas co-bombardment, we also examined the case of 100% noble gas bombardment, where one would certainly expect a large difference to the other cases. As expected, when no hydrogen was introduced into the cell, the surface hydrogen content steadily decreased under the bombardment simulations of 100% Ar, He and Ne (see Fig. 6). Also here a significant dependence on the ion energy was observed. No carbon erosion was observed in these cases, which is natural since these ions are

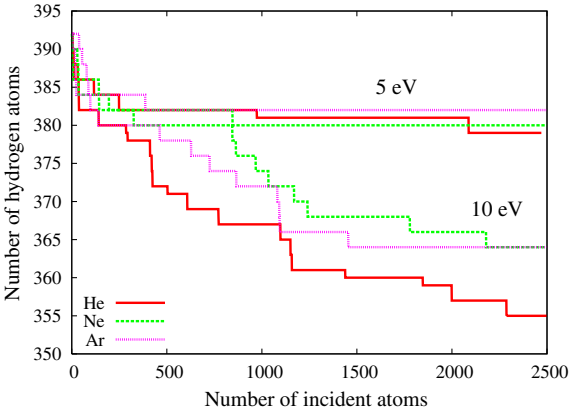

Fig. 6. Evolution of hydrogen atoms in the samples during bombardment with 100% noble gas atoms having energies of 5 (uppermost curves) and 10 eV (lower curves).

larger than hydrogen and interact almost purely repulsively with carbon. Hence they are very unlikely to enter between two carbon atoms in a way which could lead to swift chemical sputtering.

3.3. Analysis of sputtered species

Even though we stated a clear difference in the hydrogen build-up and carbon erosion yields between the 5 and the 10 eV ion bombardment simulation runs, we noticed that the C_2H_x species was the dominating sputtered species in all our simulations, both cumulative and non-cumulative runs. This is visualised in Fig. 7, where the number of different kinds of sputtered hydrocarbon molecules during different periods of the cumulative simulation runs are depicted. The analysis were done for the first 500 and the last 5000 (3000–8000) cumulative bombardment events. Under the first 500 bombardment events we saw no sputtering of larger molecules (C_xH_y with $x > 4$). The largest sputtered carbon species, $C_{18}H_x$, were seen in the 10 eV pure H, as well as H + 10% Ar cumulative ion bombardment simulations. Generally larger molecules were sputtered when the ion energy was larger.

4. Discussion

In all the 10 eV cumulative simulation runs the number of hydrogen atoms is seen to start to decrease after ~2500 events, while for 5 eV the number of hydrogen atoms in the cell remains on a constant level. The hydrogen erosion begins when no additional hydrogen supersaturation takes place and the erosion of carbon starts to become significant (thus removing hydrogen also in the eroded hydrocarbon molecules). This reveals that the erosion depends surprisingly strongly on the ion energy. The 5 eV ions can not penetrate deep into the sample and will hence form a dense surface layer which is hard to erode. The 10 eV ions will however penetrate deeper into the cell forming more loosely bound hydrocarbons (see Fig. 1(c)) which can cause the erosion of large molecules.

In our simulations the carbon erosion of the cell does not, within the statistical uncertainties, differ when different approaches are used for the energy determination. The erosion yield obtained in the 5 eV cumulative bombardment simulations where the energy was set by means of a Maxwell–Boltzmann energy distribution is calculated to be

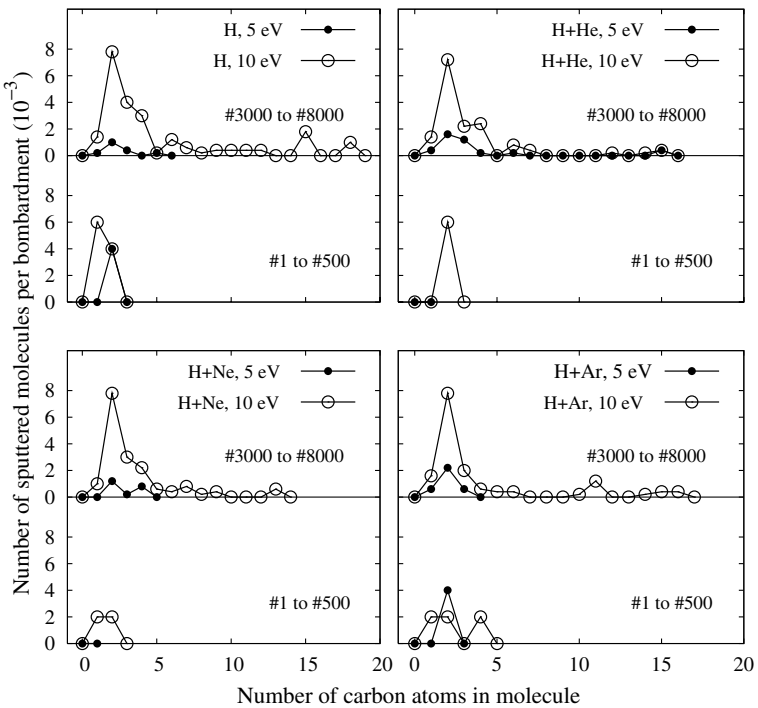

Fig. 7. Distribution of sputtered species during the first 500 frames (lower subfigure), and the last 5000 frames (upper subfigure) of cumulative simulations with only hydrogen ions as well as with hydrogen ions mixed with 10% He, 10% Ne, and 10% Ar ions. The energies of incident particles were 5 and 10 eV (mono-energetic irradiation).

$(8 \pm 2) \times 10^{-3}$ whereas the yield from the simulations with mono-energetic irradiation is $(7 \pm 2) \times 10^{-3}$.

The large differences between the hydrogen and carbon erosion yields obtained at ion energies of 5 eV and 10 eV seen in all our simulation runs, indicate that the chemical erosion of carbon in fusion reactors may be even more sensitive to the edge plasma temperature than thought previously.

By comparing the erosion yields obtained from the hydrogen and noble gas ion bombardment simulations, (see Figs. 4 and 5), we can state that there are no differences in the erosion yields from the simulations with different noble gases when the noble gas/hydrogen ratio is 0.1. Our results indicate that there is not a reason to worry that the low concentrations (<10%) of noble gases present in the divertor region would significantly alter the carbon erosion from the case with no noble gases, at least if the H and noble gas energies are the same. This can be understood to be due to the very low probability of the noble gas ions to cause swift chemical sputtering. This mechanism, which dominates the erosion in our simulations, requires penetration of a C–C bond by an incoming ion [2,4]. This penetration is easily possible for H/D/T ions, but much less likely to occur for the larger He atoms and very unlikely for heavier ions [21]. Hence the noble gas ions will not affect the erosion appreciably at low energies where physical sputtering is not possible.

In investigations of the combined interaction of energetic argon ions and thermal hydrogen atoms with plasma-deposited hydrogen layers in the low-energy region, an enhanced erosion yield (compared with the sum of the individual processes; physical sputtering due to ion bombardment and chemical erosion due to hydrogen atoms) was seen [22–24]. However, this case differs from ours in that they used thermal hydrogen, while in our case both the hydrogen and noble gases has energies in the range 1–10 eV.

By analyzing of the cumulative simulation runs, it was concluded that on average the C_2H_x species dominate the erosion of the cell. An important observation is that there occurred no erosion of larger carbon species (C_xH_y, where $x > 4$) in the first 500 cumulative bombardment events, compared with the findings from the analysis of the last 5000 bombardments in which a large amount of high-molecular weight carbon C_xH_y species (the largest being $C_{18}H_x$ species) were observed. This is reasonable, since the cell is less dense towards the end of the cumulative simulation runs than in the beginning, before the cell reaches a saturated state (see Fig. 1). Larger hydrocarbon chains, which are formed on the surface as the cumulative runs proceed beyond the saturation point, may interact with incoming ions, leading to chemical sputtering of hydrocarbon molecules when the ion induces the breaking of the bonds between the molecule and the surface.

5. Conclusions

We have performed molecular dynamics simulations of ion bombardment of amorphous hydrogenated carbon surfaces by employing an empirical hydrocarbon potential model. Cumulative simulations were run for a noble gas/hydrogen ratio of 1/10, and at ion energies of 5 and 10 eV, employing different original boxes. Within the statistical uncertainties, we do not observe any differences in the erosion yields in the simulations with different noble gases when the noble gas/hydrogen ratio is 0.1. Thus our simulations indicate that the low concentrations (<10%) of noble gases present in the divertor region would significantly alter the carbon erosion from the case with no noble gases.

On the other hand, we do observe a marked difference in the surface morphology when the ions are having different energies, leading to a large difference in the carbon erosion. This indicates that the chemical erosion of carbon in fusion reactors may be even more sensitive to the edge plasma temperature than previously assumed.

Acknowledgement

This work was supported by Association Euroatom-TEKES under the FFUSION2 programme, and the Magnus Ehrnrooth foundation. Grants of computer time from the Center for Scientific Computing in Espoo, Finland are gratefully acknowledged.

References

[1] M. Shimada, A.E. Costley, G. Federici, K. Ioki, A.S. Kukushkin, V. Mukhovatov, A. Polevoi, M. Sugihara, J. Nucl. Mater. 337–339 (2005) 808.
[2] A.V. Krasheninnikov, K. Nordlund, E. Salonen, J. Keinonen, C.H. Wu, Comput. Mater. Sci 25 (2002) 427.
[3] E. Salonen, K. Nordlund, J. Keinonen, C.H. Wu, Europhys. Lett. 52 (2000) 504.

[4] E. Salonen, K. Nordlund, J. Keinonen, C.H. Wu, Phys. Rev. B 63 (2001) 195415.
[5] E. Salonen, K. Nordlund, J. Tarus, T. Ahlgren, J. Keinonen, C.H. Wu, Phys. Rev. B 60 (1999) R14005.
[6] A. Kallenbach, A. Bard, D. Coster, R. Dux, C. Fuchs, J. Gafert, A. Herrmann, R. Schneider, J. Nucl. Mater. 266–269 (1999) 343.
[7] A. Kallenbach, A. Thoma, A. Bard, K. Behringer, K. Schmidtmann, M. Weinlichand the ASDEX upgrade team, Nucl. Fusion 38 (1998) 1097.
[8] R.D. Monk, C.A. Amiss, H.Y. Guo, G.F. Matthews, G.M. McCracken, M.F. Stamp, Phys. Scr. T81 (1999) 54.
[9] M.F. Stamp, S.K. Erents, W. Fundamenski, G.F. Matthews, R.D. Monk, J. Nucl. Mater. 290–293 (2001) 321.
[10] H. Grote, W. Bohmeyer, P. Kornejew, H.-D. Reiner, G. Fussmann, R. Schlögl, G. Weinberg, C.H. Wu, J. Nucl. Mater. 266–269 (1999) 1059.
[11] J. Roth, A. Kirschner, W. Bohmeyer, S. Brezinsek, A. Cambe, E. Casarotto, R. Doerner, E. Gauthier, G. Federici, S. Higashijima, et al., J. Nucl. Mater. 337–339 (2005) 970.
[12] D.W. Brenner, Phys. Rev. B 42 (1990) 9458.
[13] D.R. Alfonso, S.E. Ulloa, D.W. Brenner, Phys. Rev. B 49 (1994) 4948.
[14] B.J. Garrison, E.J. Dawnkaski, D. Srivastava, D.W. Brenner, Science 255 (1992) 835.
[15] R.C. Mowrey, D.W. Brenner, B.I. Dunlap, J.-W. Mintmire, C.T. White, J. Phys. Chem. 95 (1991) 7138.
[16] R.S. Taylor, B.J. Garrison, Am. Chem. Soc. 116 (1994) 4465.
[17] R.S. Taylor, B.J. Garrison, Langmuir 11 (1995) 1220.
[18] H.J.C. Berendsen, J.P.M. Postma, W.F. van Gunsteren, A. DiNola, J.R. Haak, J. Chem. Phys. 81 (1984) 3684.
[19] B.L. Doyle, W.R. Wampler, D.K. Brice, J. Nucl. Mater. 103&104 (1981) 513.
[20] J. Roth, B.M.U. Scherzer, R.S. Blewer, D.K. Brice, S.T. Picraux, W.R. Wampler, J. Nucl. Mater. 93&94 (1980) 601.
[21] K. Nordlund, E. Salonen, A.V. Krasheninnikov, J. Keinonen, Pure Appl. Chem. 78 (2006) 1203.
[22] C. Hopf, A. von Keudell, W. Jacob, Nucl. Fusion 42 (2002) L27.
[23] C. Hopf, A. von Keudell, W. Jacob, J. Appl. Phys. 94 (2003) 2373.
[24] E. Vietzke, A.A. Haasz, Physical Processes of the Interaction of Fusion Plasmas with Solids, Academic, San Diego, 1996, Chapter 4.